

- CHIRLIAN, L. E. & FRANCL, M. M. (1987). *J. Comput. Chem.* **8**, 894-905.
- CLEMENTE, D. A., BIAGINI, M. C., REES, B. & HERMANN, W. A. (1982). *Inorg. Chem.* **21**, 3741-3749.
- CLEMENTI, E. & ROETTI, C. (1974). *At. Data Nucl. Data Tables*, **14**, 177-478.
- COPPENS, P. (1989). *J. Phys. Chem.* **93**, 7979-7984.
- COPPENS, P., GURU ROW, T. N., LEUNG, P., STEVENS, E. D., BECKER, P. J. & YANG, Y. W. (1979). *Acta Cryst.* **A35**, 63-72.
- COPPENS, P. & HANSEN, N. K. (1977). *Isr. J. Chem.* **16**, 163-167.
- COPPENS, P., PAUTLER, D. & GRIFFIN, J. F. (1971). *J. Am. Chem. Soc.* **93**, 1051-1058.
- HEHRE, W. J., DITCHFIELD, R., STEWART, R. F. & POPLE, J. A. (1970). *J. Chem. Phys.* **52**, 2769-2773.
- HEHRE, W. J., STEWART, R. F. & POPLE, J. A. (1969). *J. Chem. Phys.* **51**, 2657-2664.
- HIRSHFELD, F. L. (1977). *Theor. Chim. Acta*, **44**, 129-138.
- MCLEAN, A. D. & YOSHIMINE, M. (1967). *Tables of Linear Molecule Wave Functions*. IBM J. Res. Dev. Supplement, November 1967.
- MARTIN, M., REES, B. & MITSCHLER, A. (1982). *Acta Cryst.* **B38**, 6-15.
- MASLEN, E. N. & SPACKMAN, M. A. (1985). *Aust. J. Phys.* **38**, 273-287.
- MOSS, G. (1982). In *Electron Distributions and the Chemical Bond*, edited by P. COPPENS & M. B. HALL, pp. 383-411. New York: Plenum Press.
- PEARLMAN, D. A. & KIM, S. H. (1985). *Biopolymers*, **24**, 327-357.
- SASAKI, S., FUJINO, K., TAKEUCHI, Y. & SADANAGA, R. (1980). *Acta Cryst.* **A36**, 904-915.
- STEWART, R. F. (1970). *J. Chem. Phys.* **53**, 205-213.
- STEWART, R. F. (1973). *J. Chem. Phys.* **58**, 1668-1676.
- STEWART, R. F. (1976). *Acta Cryst.* **A32**, 565-574.
- STEWART, R. F. (1977). *Isr. J. Chem.* **16**, 124-131.
- STEWART, R. F., BENTLEY, J. & GOODMAN, B. (1975). *J. Chem. Phys.* **63**, 3786-3793.
- STEWART, R. F., DAVIDSON, E. R. & SIMPSON, W. T. (1965). *J. Chem. Phys.* **42**, 3175-3187.
- YANEZ, M. & STEWART, R. F. (1978). *Acta Cryst.* **A34**, 648-651.
- YANEZ, M., STEWART, R. F. & POPLE, J. A. (1978). *Acta Cryst.* **A34**, 641-648.

*Acta Cryst.* (1991). **A47**, 29-36

## Niggli Lattice Characters: Definition and Graphical Representation

BY P. M. DE WOLFF

*Vakgroep VS-FK, Laboratorium voor Technische Natuurkunde, TU Delft, Lorentzweg 1, Postbus 5046, 2600 GA Delft, The Netherlands*

AND B. GRUBER

*Faculty of Mathematics and Physics, Charles University, Malostranské nám. 25, 11800 Prague 1, Czechoslovakia*

(Received 24 April 1990; accepted 21 August 1990)

### Abstract

An exact definition of the 44 lattice characters listed by Niggli is thoroughly discussed and is elucidated by examples. In order to represent the characters graphically, use is made of the projection of the Niggli-reduced basis vector  $\mathbf{c}$  on the  $\mathbf{a}$ ,  $\mathbf{b}$  plane. Not only is the projected end point of  $\mathbf{c}$  restricted to certain domains in the plane by the reduction rules - cf. *International Tables for Crystallography* (1987), Chapter 9.3 (Dordrecht: Kluwer) - but for given constants  $A$ ,  $B$  and  $F$  in the Niggli-reduced form this polygonal domain contains the locus of each of the characters as a vertex or an edge or the area of the polygon. For each of the cases  $a = b = c$ ,  $a = b < c$ ,  $a < b = c$  and  $a < b < c$ , nine figures fully cover all alternatives determined by five special values  $F = A/2, 0, -A/4, -A/3$  and  $-A/2$  and the four open intervals between them. Also, all normalized Buerger bases which are not Niggli-reduced bases are shown in the same figures.

### 1. Introduction

It has been shown (*International Tables*, 1987, referred to as *IT87* hereafter) that the reduced basis of any given crystal lattice can be elucidated graphically by the perpendicular projection of the reduced basis vector  $\mathbf{c}$  upon the  $\mathbf{a}$ ,  $\mathbf{b}$  plane. Because of the rules for cell reduction, only points within certain regions in that plane are allowed as a possible projected end point of  $\mathbf{c}$ ,  $\mathbf{a}$  and  $\mathbf{b}$  being considered as given vectors. Drawings of the  $\mathbf{a}$ ,  $\mathbf{b}$  plane, showing these regions for only a limited number of typical cases, fully illustrate all rules of cell reduction.

The reduced cell which we here refer to is the cell introduced by Niggli (1928). Since some other types of reduced cell have been discussed recently (Gruber, 1989), we shall denote it further as the 'Niggli cell', and its normalized basis as the 'Niggli basis'.

Closely related to Niggli cells are the lattice characters, which constitute a classification of lattices based mainly on lattice symmetry expressed in the

Niggli-cell parameters. Therefore, as a logical extension of the above illustration principle, one could use such projection drawings in order to depict the characters as well. The present paper shows that all 44 lattice characters can indeed be portrayed in this manner. Moreover, all non-Niggli Buerger cells are indicated in the same figures.

Clear definitions of Niggli's lattice characters in the existing literature are scarce - usually they are just listed in an unexplained table. Therefore, we shall first discuss this definition in a way which we hope will contribute to the understanding of the inherent simplicity of the lattice-character concept.

## 2. Definition of lattice characters

The 'lattice character' has been introduced by Niggli (1928). It yields a classification of lattices which is much more refined than that offered by the Bravais types. Niggli defined it (not exhaustively, as we shall see) by stating that two lattices have the same character when the 'necessary relations' between the parameters  $A, \dots, F$  of their Niggli bases are identical. We shall call this condition the 'Niggli criterion'.

The Niggli basis (*cf.* IT87) consists of three edges  $\mathbf{a}$ ,  $\mathbf{b}$  and  $\mathbf{c}$  of a Buerger cell. This means (Buerger, 1957; IT87) that

$$a + b + c = \text{minimum} \quad (1)$$

for the given lattice. It is normalized with regard to labelling of the cell edges by  $a$ ,  $b$  and  $c$ , *cf.* the conditions (2), (4) and (6) below. The ensuing 'normalized form' of a Buerger cell is the set of the six numbers  $A = \mathbf{a} \cdot \mathbf{a}$ ,  $B = \mathbf{b} \cdot \mathbf{b}$ ,  $C = \mathbf{c} \cdot \mathbf{c}$ ,  $D = \mathbf{b} \cdot \mathbf{c}$ ,  $E = \mathbf{a} \cdot \mathbf{c}$  and  $F = \mathbf{a} \cdot \mathbf{b}$ . This form is a complete description of the lattice, but it is not always unique because some lattices have two or more non-congruent Buerger cells, *cf.* Gruber (1973).

However, for any lattice there is always just one Buerger cell - called 'Niggli-reduced cell' or just 'Niggli cell' - which satisfies a certain set of 'special conditions' for the symbols  $A, \dots, F$  (Eisenstein, 1851; Niggli, 1928; IT87). Gruber (1989) has shown that it can be given a geometric interpretation: if there are two or more Buerger cells, one of them has a larger 'deviation' (sum of the absolute departures of the three angles from  $90^\circ$ ) than the other(s), and this is the Niggli cell. Clearly, the normalized form of the corresponding 'Niggli basis' is a unique characteristic of the lattice. In what follows, the parameters  $A, \dots, F$  always refer to this 'Niggli form'.

The 'necessary relations' are the equations in  $A, \dots, F$  following from the point-group symmetry of the lattice. Their number varies from 0 (triclinic) to 5 (cubic). If the above 'Niggli criterion' for two lattices to have the same character is satisfied, they have the same Bravais type as well (de Wolff, 1988).

This is why characters can be used to find the Bravais type from a given Niggli form.

As a first example, consider a primitive tetragonal ( $tP$ ) lattice. The lattice symmetry produces four equations. Expressed in conventional lattice parameters (subindex  $c$ ), these equations are:  $a_c = b_c$ ,  $\alpha_c = \beta_c = \gamma_c = 90^\circ$ . So if the reduced basis coincides with the conventional basis (which occurs when  $c_c > a_c$ ) the four necessary relations are  $A = B$  and  $D = E = F = 0$ . However, when  $c_c < a_c$  the normalization rule

$$A \leq B \leq C \quad (2)$$

prescribes a different labelling of the cell edges, with  $\mathbf{a}$  along the fourfold axis. Then the necessary relations are  $B = C$  and  $D = E = F = 0$ . Because this set differs from the first, these two kinds of  $tP$  lattices have two separate characters. They have nos. 11 and 21 in the enumeration of sets of relations for 44 characters by Mighell & Rodgers (1969). Mighell's table is essentially identical to the table by Niggli (1928) except that the characters are numbered, in the sequence in which they are listed by Niggli. It also lists the Bravais type for each character. This numbered table will be called the 'Niggli table'. Obviously, if in the same range of lattices one puts  $a_c = c_c$ , the lattice is no longer of type  $tP$  but it becomes the cubic primitive type  $cP$ . This has a fifth symmetry relation. It forms a separate character by itself, no. 3, with  $A = B = C$  and  $D = E = F = 0$ .

To find the character of a lattice one obviously has to first find the values of its parameters  $A, \dots, F$  and then to check which of the 44 sets of relations in the Niggli table is fulfilled by these values. Suppose the lattice is of the  $cP$  type just dealt with, then clearly its parameters  $A, \dots, F$  fit the five relations just mentioned. However, they also fulfil the four relations given above for no. 11 since these do not restrict  $C$ ; and also those for no. 21 which leave  $A$  entirely free. Actually, there are several more characters of which the relations are obeyed although they are not the true solution. We shall call them 'subcharacters' of the given lattice. As will be shown presently, it is not difficult to distinguish them from the true character.

It may seem strange that the 'necessary relations' are not supplemented by inequalities which would completely delimit the range of each character. For instance, if to the above relations for no. 11 the inequality  $B < C$  is added they no longer overlap with those for no. 3. The reason for not doing so is that such limiting inequalities - though very simple in this case - are extremely complicated for characters of lower symmetry, where the relations themselves are often unrecognizable as symmetry relations.

Since the relations stem from lattice symmetry, each subcharacter must correspond to a holohedric subgroup (here  $4/mmm$ ) of the symmetry (here  $m\bar{3}m$ ) of the given lattice. Accordingly, the latter's

set of necessary relations contains those of all subcharacters as subsets. So the true character is always the one which comes first when the solutions are ordered in the following sequence:

cubic	(5 relations);	
hexagonal, tetragonal or trigonal	(4 relations);	
orthorhombic	(3 relations);	(3)
monoclinic	(2 relations);	
triclinic	(0 relations).	

There is of course always a single solution with the largest number of relations. Among the subcharacters, however, two or more characters belonging to the same system may occur. The following example will serve to elucidate these facts:

Suppose the lattice is given by its Niggli form:

$$(ABCDEF) = (2, 2, 3, -1, -1, 0).$$

Going through the Niggli table, one finds agreement for the following entries:

14, 15, 16, 17, 37, 41, 42, 43, 44,  
with Bravais types:  
*mC tI oF mC mC mC oI mC aP.*

One sees immediately that the highest symmetry (tetragonal) occurs for no. 15 only; this is the true character of the given lattice.

### 3. The cell-type criterion

Apart from the 'necessary relations' criterion discussed above, Niggli tacitly used an additional criterion for identifying characters. It has to do with the normalizing rules for *D*, *E* and *F*: the cell edges are labelled in such a way that these three parameters are

$$\text{either all positive (cell type I)} \quad (4a)$$

$$\text{or all non-positive (cell type II)}. \quad (4b)$$

The additional criterion for two lattices to have the same character is that their Niggli cells be of the same type (de Wolff, 1988). This 'cell-type criterion' causes a character to be split in two when the corresponding relations between *A*, ..., *F* fit lattices with reduced cells of both types I and II. The splitting of a character is, as it were, inherited by each of its subcharacters, since the latter's range of lattices includes that of the former. So one can easily find the split cases by looking for them in the higher symmetries first. One finds that among these only the range of rhombohedral lattices for which  $A = B = C$  and  $D = E = F$  splits up, *viz* into nos. 2 (type I) and 4 (type II). These characters have no orthorhombic and just two monoclinic subcharacters each, *viz* nos. 10 and 20 for

no. 2, and nos. 14 and 25 for no. 4. As the last generation their triclinic subcharacters nos. 31 and 44 appear; *cf.* the following table:

Type I	Type II	Relations	Bravais type
2	4	$A = B = C, D = E = F$	<i>hR</i>
10	14	$A = B, D = E$	<i>mC</i>
20	25	$B = C, E = F$	<i>mC</i>
31	44	None	<i>aP.</i>

Each of the remaining 36 sets of relations defines cells of either type I only or type II only. This brings the total number of characters to 44, instead of the 40 which would follow from the Niggli criterion alone. Since one of us has stated (de Wolff, 1988) that Niggli had missed some characters, it should be stressed that Niggli in his original table (Niggli, 1928) listed all 44; the remark referred to his figures only.

The generation of the above eight characters from four sets of relations in no way interferes with the above procedure for character determination, except that the cell type has to be specified as an extra condition.

### 4. 'First-hit' checking sequences

The sequence in which the characters (or rather, sets of relations) were listed by Niggli (1928) was intended to allow identification of the character of a lattice by the first set of relations which is fulfilled by the lattice's Niggli-form parameters. From what has been said in § 2 about the relation with lattice symmetry, it will be clear that such a 'first-hit' sequence would already have been obtained by putting the characters in five successive groups of decreasing symmetry; this would make checking more difficult than Niggli's

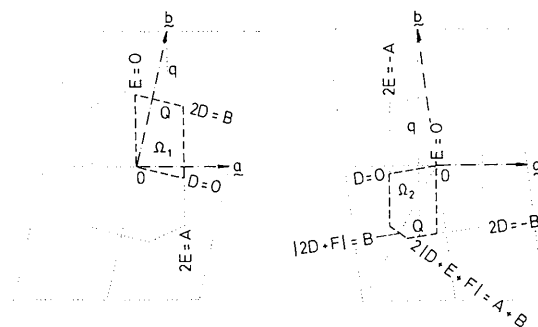


Fig. 1. The regions  $\Omega_1$  and  $\Omega_2$  in the *a*, *b* plane, allowed by the minimum condition (1) and by the normalizing condition (4a, b) for the projection *P* of the end point of the vector *c* - assumed to head upwards - on this plane, for Buerger cells of type I (left) and II (right). The same regions are also indicated in all plots of Fig. 2 which show that their general shape is not greatly affected by variation of *B/A* and *F/A* from the arbitrary values chosen here. For several conditions in the Niggli table, the lines and the equations in *D* and *E* to which they correspond are shown (*q* is the line  $E = F$ ).

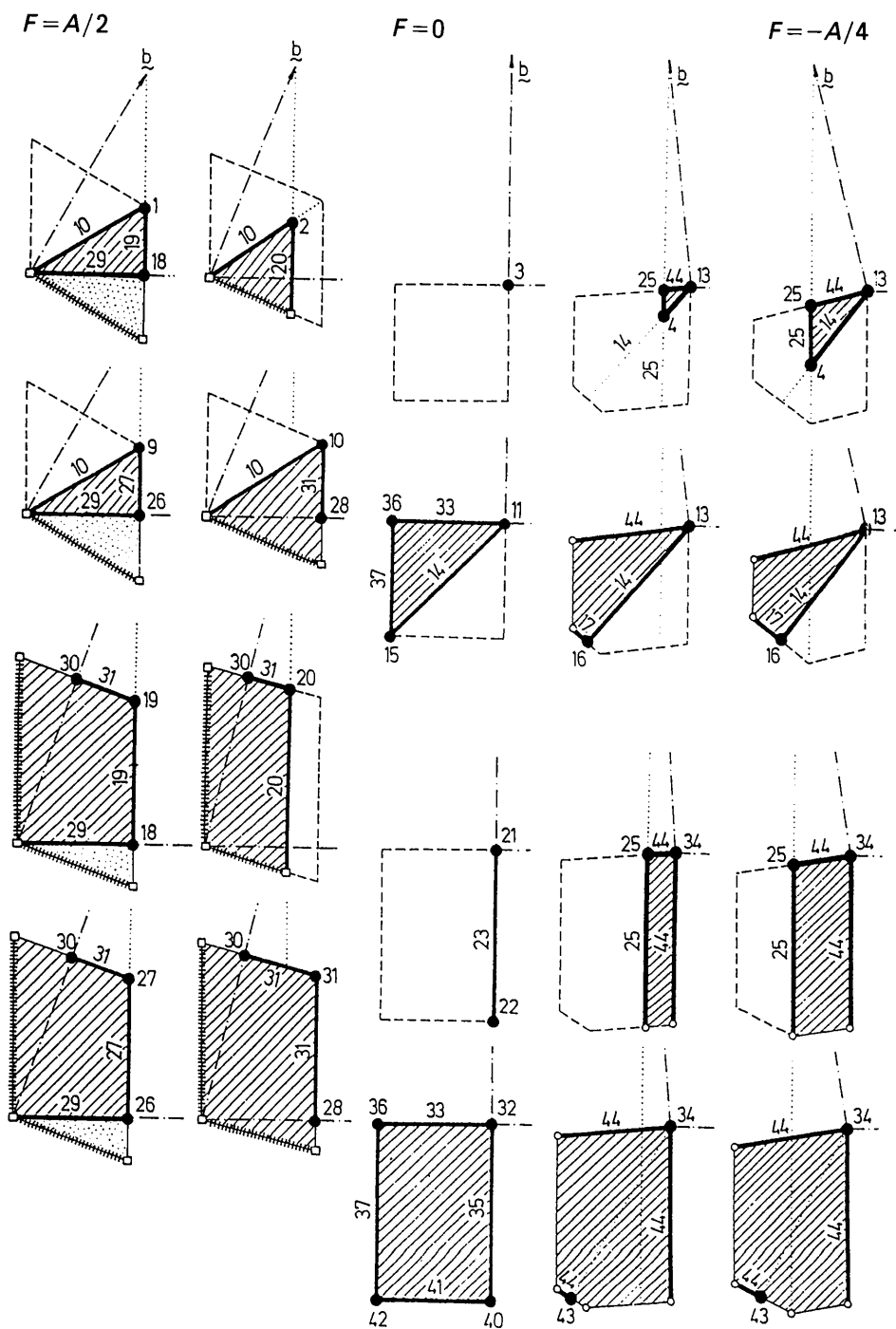


Fig. 2. The 44 lattice characters and all normalized non-Niggli Buerger cells, illustrated in the  $a, b$  plane. The four rows correspond to the partition (5) as indicated at the far right. In each row the value of  $F/A$  decreases from left to right; special values are marked on top, and the plots in columns not thus marked apply to the open intervals in between. The vector  $a$  is identically the same for all 36 plots and is shown in full only in the last column. The vector  $b$  is shown in full in the first row; in the other three only its direction is indicated. Whereas  $b = a$  for the second row (just as in the first row),  $b > a$  in the third and fourth rows. This is not directly seen in the figure. Graphical symbols are explained in Table 1. The character of lattices corresponding to points  $P$  in the hatched areas is no. 31 in the first and second column, and no. 44 in the remaining columns. Wherever this area number also applies to a boundary segment it is printed alongside; similarly for any line segment and its end point(s) wherever they share a character.

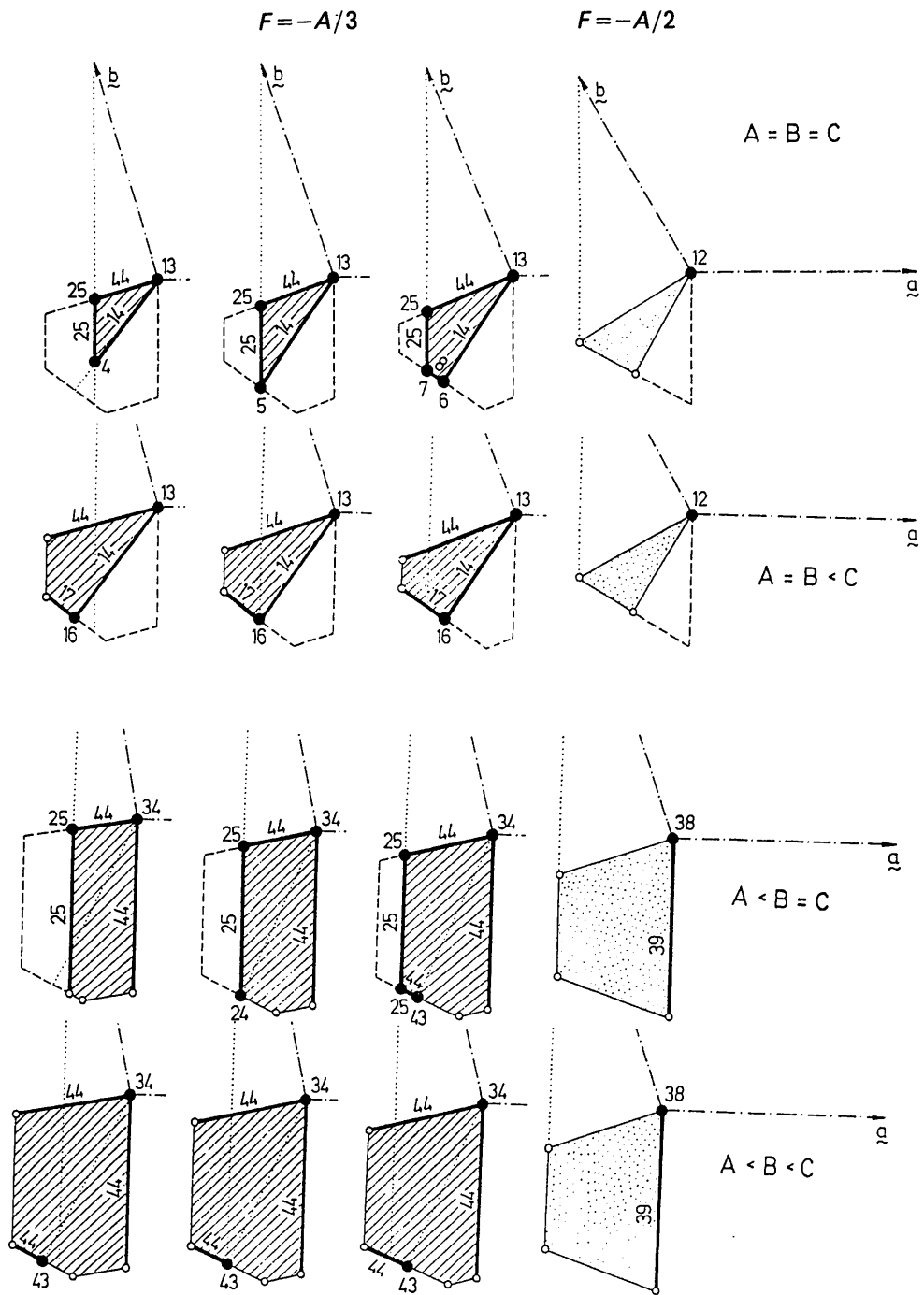


Fig. 2 (cont.)

grouping by cell type and by the equalities (if any) between  $A$ ,  $B$  and  $C$ .

Gruber (1980) has noted that the Niggli table does not fully achieve the intended efficiency (for instance, in the above example, the correct character has no. 15, not the lowest number, 14). He has proposed some interchanges to make it a real 'first-hit' table, and these have been incorporated in the 1983 and later editions of *International Tables*, which however retain the original character numbers, cf. Table 2.

Even within the Niggli type of grouping, the 'first-hit' sequence is not unique. We can, for instance, change the order of the last 12 entries (now 40-35-36-33-38-34-42-41-37-39-43-44) into 36-33-38-34-40-35-42-37-39-41-43-44 and still hit the correct character first.

### 5. Graphical representation

As announced in § 1, we consider a plane containing the vectors  $\mathbf{a}$  and  $\mathbf{b}$  of the Niggli basis. The vector  $\mathbf{c}$  is supposed to head upwards. All three vectors begin at the same origin  $O$ . We are interested in the perpendicular projection  $P$  of the end point of  $\mathbf{c}$  on the  $\mathbf{a}$ ,  $\mathbf{b}$  plane. Our aim is to ascertain the relation between the position of  $P$  and the character of the lattice.

The general shape of this projected situation is illustrated in Fig. 1. Here it is important to realize that all points  $P$  of any line perpendicular to  $\mathbf{a}$  represent lattices with the same value of  $\mathbf{c} \cdot \mathbf{a}$ , that is, of  $E$ . This value is proportional to the line's distance  $x$  from  $O$ ; it is  $E = (x/a)A$ , provided  $x$  is given the appropriate sign, namely, positive in the direction of  $\mathbf{a}$ . Similarly, a line perpendicular to  $\mathbf{b}$ , at a distance  $y$  from  $O$ , represents all lattices with  $D = (y/b)B$ .

It follows that the projection drawing can be seen as a plot of  $D$  and  $E$  as coordinates on (in general) oblique axes, marked  $D=0$  and  $E=0$  in Fig. 1, for fixed  $A$ ,  $B$  and  $F$ . Then the only Niggli parameter not defined by the position of  $P$  in the plot is  $C$ .

By the minimum condition (1), the region allowed for  $P$  is a polygon bounded by pairs of lines perpendicular to  $\mathbf{a}$  and  $\mathbf{b}$ , at distances of  $a/2$  and  $b/2$  from  $O$  (in Fig. 1 they are marked by their equation  $2D = B$  or  $-B$ , and  $2E = A$  or  $-A$ ) and by another pair of lines perpendicular either to  $\mathbf{a} + \mathbf{b}$  at a distance  $|\mathbf{a} + \mathbf{b}|/2$  from  $O$  (when  $F < 0$ ) or to  $\mathbf{a} - \mathbf{b}$  at a distance  $|\mathbf{a} - \mathbf{b}|/2$  from  $O$  (when  $F > 0$ ). Moreover, from this polygon only one quadrant remains because of the normalizing conditions (4a, b). This quadrant is a tetragon when  $F \geq 0$  and a pentagon when  $F < 0$ . We shall denote it by  $\Omega_1$  and  $\Omega_2$ , respectively. Both are shown in Fig. 1 and again in the plots for all cases of Fig. 2. Point  $P$  may lie on their boundaries, but not on the  $D$  and  $E$  axes in  $\Omega_1$ , when  $F > 0$ , because of (4a).

For given values of  $A$ ,  $B$  and  $F$  the dependence of characters on the 'invisible' parameter  $C$  is so fortu-

Table 1. Key to the graphical symbols used in Fig. 2

(a)	●	—	▨	Points, lines and areas corresponding to Niggli cells
(b)	○	—	▩	Points, lines and areas corresponding to non-Niggli Buerger cells
(c)	□			Points and lines of the boundary of $\Omega_1$ , which are excluded for $P$ by (4a)
(d)		-----		The boundary of $\Omega_1$ and $\Omega_2$ , unless denoted otherwise
(e)		----->		The vectors $\mathbf{a}$ , $\mathbf{b}$
(f)		.....		Auxiliary constructions

nate that it can be represented by only four separate plots which are unique, i.e. where each point  $P$  always represents just one character. These plots are determined by the conditions

$$A = B = C; A = B < C; A < B = C; \quad (5)$$

and  $A < B < C$ .

[Although these conditions strongly resemble the four subheadings of the Niggli table, it should be stressed that they are really quite different. Conditions (5) are mutually exclusive; the subheadings are not.]

The conditions in the body of the Niggli table all correspond to points or straight lines in the plot. By way of example, some of the lines are shown in Fig. 1 together with the relevant equation.

To finish this explanation of Fig. 2, we observe that there is one more normalizing condition for reduced bases:

$$\text{if } A = B, \text{ then } |D| \leq |E| \quad (6a)$$

$$\text{if } B = C, \text{ then } |E| \leq |F|. \quad (6b)$$

Clearly, (6a) means that the regions  $\Omega_1$  and  $\Omega_2$  are halved symmetrically by the line  $D = E$  in the first two cases of (5). In the first and third cases, (6b) causes them to be truncated by the line  $q$  ( $E = F$ ).

For each of the four cases (5), Fig. 2 shows a row of nine different character plots, covering the full range of all six parameters  $A, \dots, F$ . This is achieved as follows: We consider  $A$  as an uninteresting scale parameter;  $B/A$  and the invisible  $C$  are accounted for by the partition (5). For the plots in the third and fourth row of Fig. 2, an arbitrary value of  $B/A > 1$  has been chosen. Any other value in this range would of course yield a different plot - but it would be equivalent to the one shown. Here, 'equivalent' means that it would contain the same characters, their domains (points, line segments or areas) delimited in exactly the same way by the corresponding vertices and edges of  $\Omega_1$  and  $\Omega_2$ , as well as by the line  $E = F$  mentioned above.

Since  $D$  and  $E$  are the variable coordinates of each plot, the only remaining parameter is  $F$ . It has 'special' values  $A/2$ ,  $0$ ,  $-A/3$  and  $-A/2$ , called 'special' because, for one or more of the cases (5), the corresponding plots are not equivalent (in the sense just defined) to those for values in the adjoining  $F/A$

Table 2. The parameters  $D = \mathbf{b} \cdot \mathbf{c}$ ,  $E = \mathbf{a} \cdot \mathbf{c}$  and  $F = \mathbf{a} \cdot \mathbf{b}$  of the 44 lattice characters ( $A = \mathbf{a} \cdot \mathbf{a}$ ,  $B = \mathbf{b} \cdot \mathbf{b}$ ,  $C = \mathbf{c} \cdot \mathbf{c}$ )

The character of a lattice given by its Niggli form is the first one which agrees when the 44 entries are compared with that form in the sequence given below. Such a logical order is not always obeyed by the widely used character numbers (first column) which therefore show some reversals, e.g. 4 and 5.

No.	Type	$D$	$E$	$F$	Lattice symmetry	Bravais type†	Transformation to a conventional basis
<i>A = B = C</i>							
1	I	$A/2$	$A/2$	$A/2$	Cubic	$cF$	$\bar{1}\bar{1}1/1\bar{1}\bar{1}/\bar{1}\bar{1}1$
2	I	$D$	$D$	$D$	Rhombohedral	$hR$	$\bar{1}\bar{1}0/\bar{1}01/\bar{1}\bar{1}\bar{1}$
3	II	0	0	0	Cubic	$cP$	100/010/001
5	II	$-A/3$	$-A/3$	$-A/3$	Cubic	$cI$	101/110/011
4	II	$D$	$D$	$D$	Rhombohedral	$hR$	$\bar{1}\bar{1}0/\bar{1}01/\bar{1}\bar{1}\bar{1}$
6	II	$D^*$	$D$	$F$	Tetragonal	$tI$	011/101/110
7	II	$D^*$	$E$	$E$	Tetragonal	$tI$	101/110/011
8	II	$D^*$	$E$	$F$	Orthorhombic	$oI$	$\bar{1}\bar{1}0/\bar{1}0\bar{1}/0\bar{1}\bar{1}$
<i>A = B, no conditions on C</i>							
9	I	$A/2$	$A/2$	$A/2$	Rhombohedral	$hR$	100/ $\bar{1}\bar{1}0/\bar{1}\bar{1}\bar{3}$
10	I	$D$	$D$	$F$	Monoclinic	$mC$	110/ $\bar{1}\bar{1}0/00\bar{1}$
11	II	0	0	0	Tetragonal	$tP$	100/010/001
12	II	0	0	$-A/2$	Hexagonal	$hP$	100/010/001
13	II	0	0	$F$	Orthorhombic	$oC$	110/ $\bar{1}\bar{1}0/001$
15	II	$-A/2$	$-A/2$	0	Tetragonal	$tI$	100/010/112
16	II	$D^*$	$D$	$F$	Orthorhombic	$oF$	$\bar{1}\bar{1}0/\bar{1}\bar{1}0/112$
14	II	$D$	$D$	$F$	Monoclinic	$mC$	110/ $\bar{1}\bar{1}0/001$
17	II	$D^*$	$E$	$F$	Monoclinic	$mC$	$\bar{1}\bar{1}0/110/\bar{1}0\bar{1}$
<i>B = C, no conditions on A</i>							
18	I	$A/4$	$A/2$	$A/2$	Tetragonal	$tI$	$0\bar{1}\bar{1}/1\bar{1}\bar{1}/100$
19	I	$D$	$A/2$	$A/2$	Orthorhombic	$oI$	$\bar{1}00/0\bar{1}\bar{1}/\bar{1}\bar{1}1$
20	I	$D$	$E$	$E$	Monoclinic	$mC$	011/01 $\bar{1}/\bar{1}00$
21	II	0	0	0	Tetragonal	$tP$	010/001/100
22	II	$-B/2$	0	0	Hexagonal	$hP$	010/001/100
23	II	$D$	0	0	Orthorhombic	$oC$	011/0 $\bar{1}\bar{1}/100$
24	II	$D^*$	$-A/3$	$-A/3$	Rhombohedral	$hR$	121/0 $\bar{1}\bar{1}/100$
25	II	$D$	$E$	$E$	Monoclinic	$mC$	011/0 $\bar{1}\bar{1}/100$
<i>No conditions on A, B, C</i>							
26	I	$A/4$	$A/2$	$A/2$	Orthorhombic	$oF$	100/ $\bar{1}20/\bar{1}0\bar{2}$
27	I	$D$	$A/2$	$A/2$	Monoclinic	$mC$	$\bar{1}20/\bar{1}00/0\bar{1}\bar{1}$
28	I	$D$	$A/2$	$2D$	Monoclinic	$mC$	$\bar{1}00/\bar{1}0\bar{2}/010$
29	I	$D$	$2D$	$A/2$	Monoclinic	$mC$	100/ $\bar{1}20/00\bar{1}$
30	I	$B/2$	$E$	$2E$	Monoclinic	$mC$	010/01 $\bar{2}/\bar{1}00$
31	I	$D$	$E$	$F$	Triclinic	$aP$	100/010/001
32	II	0	0	0	Orthorhombic	$oP$	100/010/001
40	II	$-B/2$	0	0	Orthorhombic	$oC$	0 $\bar{1}0/01\bar{2}/\bar{1}00$
35	II	$D$	0	0	Monoclinic	$mP$	0 $\bar{1}0/\bar{1}00/00\bar{1}$
36	II	0	$-A/2$	0	Orthorhombic	$oC$	100/ $\bar{1}0\bar{2}/010$
33	II	0	$E$	0	Monoclinic	$mP$	100/010/001
38	II	0	0	$-A/2$	Orthorhombic	$oC$	$\bar{1}00/120/00\bar{1}$
34	II	0	0	$F$	Monoclinic	$mP$	$\bar{1}00/00\bar{1}/0\bar{1}0$
42	II	$-B/2$	$-A/2$	0	Orthorhombic	$oI$	$\bar{1}00/0\bar{1}0/112$
41	II	$-B/2$	$E$	0	Monoclinic	$mC$	01 $\bar{2}/0\bar{1}0/\bar{1}00$
37	II	$D$	$-A/2$	0	Monoclinic	$mC$	10 $\bar{2}/100/010$
39	II	$D$	0	$-A/2$	Monoclinic	$mC$	$\bar{1}20/\bar{1}00/00\bar{1}$
43	II	$D^\dagger$	$E$	$F$	Monoclinic	$mI$	$\bar{1}00/\bar{1}\bar{1}\bar{2}/0\bar{1}0$
44	II	$D$	$E$	$F$	Triclinic	$aP$	100/010/001

\*  $2|D + E + F| = A + B$ .

† As footnote \* plus:  $|2D + F| = B$ .

‡ The capital letter of the symbols in this column indicates the centring type of the cell as obtained by the transformation in the last column. For this reason the standard symbols  $mS$  and  $oS$  are not used here.

intervals. Moreover, a similar although very slight discontinuity occurs at  $F = -A/4$ ; therefore we treat this as a special value as well. Within any one of the four open intervals of  $F$  in between the special values, only mutually equivalent plots occur. So in each row of Fig. 2 they figure as a single plot, for which  $F/A$  has an arbitrary value in the relevant interval.

In order to facilitate orientation in the plots of Fig. 2, the region  $\Omega_1$  or  $\Omega_2$  is indicated in each of them. The points, lines or areas corresponding to each

character are indicated by the graphical symbols explained in Table 1. This table also explains symbols used for normalized non-Niggli Buerger cells, cf. Gruber (1973), all of which are illustrated in Fig. 2. Table 2 is a reproduction of Table 9.3.1 of *IT87*.

Note that the above special values of  $F/A$  can be easily recognized by considering the position of the vertical  $q$  through the end point of  $\mathbf{b}$  (equation  $E = F$ ) with respect to the vertices of  $\Omega_1$  or  $\Omega_2$ , see point  $Q$  in Fig. 1.

The authors express their gratitude to Mrs J. Jelínková for preparing Figs. 1 and 2.

#### References

- BUERGER, M. J. (1957). *Z. Kristallogr.* **109**, 42–60.  
 EISENSTEIN, G. (1851). *J. Math. Crelle*, **41**, 141–190.  
 GRUBER, B. (1973). *Acta Cryst.* **A29**, 433–440.  
 GRUBER, B. (1980). Private communication.  
 GRUBER, B. (1989). *Acta Cryst.* **A45**, 123–131.  
*International Tables for Crystallography* (1987). Vol. A, 2nd. ed. Ch. 9.3, especially Table 9.3.1. Dordrecht: Kluwer.  
 MIGHELL, A. D. & RODGERS, J. R. (1969). *International Tables for X-ray Crystallography*, Vol. I, 3rd ed., pp. 530–535. Birmingham: Kynoch Press.  
 NIGGLI, P. (1928). *Handbuch der Experimentalphysik*, Vol. 7, Part 1, pp. 108–176. Leipzig: Akademische Verlagsgesellschaft.  
 WOLFF, P. M. DE (1988). *Comput. Math. Appl.* **16**, 487–492.

*Acta Cryst.* (1991). **A47**, 36–39

## Determination of the Sign of a Dislocation in a ZnTe Crystal by Convergent-Beam Electron Diffraction\*

BY F. NIU, R. WANG AND G. LU

*Department of Physics, Wuhan University, 430072 Wuhan, People's Republic of China*

(Received 22 May 1990; accepted 29 August 1990)

### Abstract

The twist and distortion of diffraction fringes in a convergent-beam electron diffraction pattern, caused by a dislocation in a ZnTe crystal, have been studied systematically. It has been found that the sense of such a twist reverses when the beam crossover changes from one side of the specimen to the other. From a qualitative consideration, it has been concluded that the diffraction fringes on the side pointed to by the vector  $\mathbf{u} \times \mathbf{c}$  are shifted along  $\mathbf{b}$ . This phenomenon can be used to determine the sign of the Burgers vector of a dislocation.

### 1. Introduction

Recently, progress has been made in studying dislocations in crystals by means of convergent-beam electron diffraction (CBED). After the initial work of Carpenter & Spence (1982), it was proposed that diffraction fringes in the central disc may be used to determine the Burgers vector of a dislocation (Cherns & Preston, 1986; Cherns, Kiely & Preston, 1988; Tanaka, Terauchi & Kaneyama, 1988). Wen, Wang & Lu (1989) noticed that the zeroth-order Laue-zone (ZOLZ) pattern in the central disc is convenient for studying the geometry of dislocations, and they made extensive computer simulations to verify its feasibility in various dislocation cases (Lu, Wen, Zhang & Wang, 1990). These authors also pointed out that the position of the convergent-beam crossover relative to the specimen can greatly influence the ZOLZ pattern, and thus it is important in determining the sign of

the Burgers vector of a dislocation. In this paper, we report the investigation of the influence of dislocations in a II–VI semiconductor compound ZnTe crystal on diffraction fringes in the central discs in defocused CBED patterns. We make clear that both the value and the sign of  $\Delta f$  can influence the detail characteristics of the distorted diffraction fringes.

### 2. Experiments

A ZnTe polycrystal was compressed along the crystal growing axis. The compressed crystal was sliced with a wire saw to about 200  $\mu\text{m}$ , and the surface normal of the slices is about 45° from the growing axis. The deformed ZnTe was ground and polished mechanically down to about 40  $\mu\text{m}$ . The specimens were then ion-beam thinned for the observation of transmission electron microscopy (TEM).

The CBED experiments were carried out on a JEM-100CX(II) transmission electron microscope by lowering the specimen stage. The beam crossover can be moved above or below the specimen a distance  $\Delta f$  by changing the objective-lens current with the FOCUS knob. Then the condenser-lens current is adjusted to form a pattern consisting of sharp spots under the imaging mode. Each spot in this pattern corresponds to an image (bright-field image or dark-field image). The defocus value  $\Delta f$  is measured using the distance  $R$  of a dark-field image from the bright-field image (the center spot):  $\Delta f = R/(2\theta_B)$  with  $\theta_B$  being the Bragg angle of this dark-field spot. In this paper, the positive sense of  $\Delta f$  is taken downwards from the specimen along the optical axis. Owing to a defocus illumination, the shadow image of a dislocation and the distortion of diffraction fringes can be observed simultaneously.

\* Project supported by the National Natural Science Foundation of China.